Polymer Chemistry

ROYAL SOCIETY OF CHEMISTRY

PAPER

View Article Online
View Journal | View Issue

Check for updates

Cite this: *Polym. Chem.*, 2021, **12**, 4104

Received 9th June 2021,
Accepted 16th June 2021

DOI: 10.1039/d1py00781e

rsc.li/polymers

Photo-liberated amines for *N*-carboxyanhydride (PLANCA) ring-opening polymerization†

Sofia L. Goodrich,‡ Megan R. Hill,‡ Rebecca A. Olson and Brent S. Sumerlin *

The polymerization of *N*-carboxyanhydrides (NCAs) affords access to a vast array of synthetic polypeptides with tunable molecular weights, functionalities, and architectures. The use of light to achieve spatiotemporal control over these polymerizations could expand their applicability to a variety of areas, including 3D printing and photolithography. In this report we utilized 2-(2-nitrophenyl)propyloxycarbonyl (NPPOC) as a photoprotecting group to cage a primary amine initiator that is activated upon UV irradiation. NPPOC photocages underwent quantitative deprotection and afforded better polymerization control compared to previously reported photocaged amines for NCA polymerizations. Furthermore, the addition of a small equivalence of base enhanced the control and resulted in polymers with lower dispersities. Overall, this method advances photo-controlled polypeptide synthesis by demonstrating high chain-end fidelity, efficient chain extension, and the ability to synthesize block copolymers.

Introduction

Light-mediated polymerization has emerged as a powerful tool in the synthesis of advanced materials. The spatial and temporal control imparted by light makes it an appealing external source of energy for initiation. While growth in the area of photocontrolled polymerization has recently gained momentum,[1–3] photoinitiated polymerization has been used for many years in commercial products such as adhesives, inks, and coatings, as well as in technologies, such as photolithography and additive manufacturing.[4–6] While much of the work previously reported on photocontrolled and photoinitiated systems has focused on the radical or cationic polymerization of vinyl monomers, expanding the scope to the synthesis of biopolymers like polypeptides could lead to materials that are both biocompatible and degradable.[7]

Ring-opening polymerization (ROP) of *N*-carboxyanhydrides (NCAs) has become the leading route to synthesize high molecular weight synthetic polypeptides.[8,9] Recent advancements in NCA ROP have provided access to well-defined chain-end[10] and side-chain[11,12] functional polypeptides, polymers with unique and stable 3D secondary structures,[13,14] and stimuli-responsive "smart" polypeptides.[15] In addition, many examples of light-responsive NCA-derived polymers have been reported, predominantly relying on the photocaging of NCA side-chains with *o*-nitrobenzyl groups to impart structural, charge, or solubility changes of the resulting polymer under light irradiation.[16–18] Only recently has photoinitiated NCA ROP emerged.

The first example of photoinitiated NCA ROP was reported by Heise and coworkers, in which two photocaged cyclohexyl amine initiators ((2,6-dinitrobenzyl cyclohexylcarbamate) and (4,5-dimethoxy-2-nitrobenzylcyclohexylcarbamate)) acted as dormant, light-labile initiators (Fig. 1A).[19] Upon irradiation, cyclohexylamine was released to initiate NCA ROP, thereby imparting temporal control over the polymerization. The same group extended this technique to grow polypeptides from surfaces, using silicon wafers grafted with photocleavable 4,5-dimethoxy-2-nitrobenzylcyclohexylcarbamate.[20] Dong *et al.* also reported light-initiated NCA ROP *via* a photocaged lysine NCA (N_ε-(*o*-nitrobenzyloxycarbonyl)-L-lysine-NCA and N_ε-(1-(2-nitrophenyl)ethoxycarbonyl)-L-lysine-NCA) as a means of producing hyperbranched polypeptides (Fig. 1B).[21,22] Upon light irradiation, the unmasked lysine NCA acted as an inimer (initiator and monomer) to produce branched polylysine. These reports were instrumental in demonstrating the promise of photopolymerization for polypeptide synthesis. However, these photoinitiated systems required either extended irradiation times to achieve efficient deprotection, or full photodeprotection was not realized. The slow release of initiating amines and incomplete deprotection affects initiation and polymerization kinetics, as well as control over molecular weight. For example, Heise *et al.* demonstrated that increasing irradiation time resulted in lower molecular weight and increased molecular weight dispersity, presumably due to the

---

George & Josephine Butler Polymer Research Laboratory, Center for Macromolecular Science & Engineering, Department of Chemistry, University of Florida, PO Box 117200, Gainesville, Florida 32611, USA. E-mail: sumerlin@chem.ufl.edu

† Electronic supplementary information (ESI) available. See DOI: 10.1039/d1py00781e

‡ These authors contributed equally.

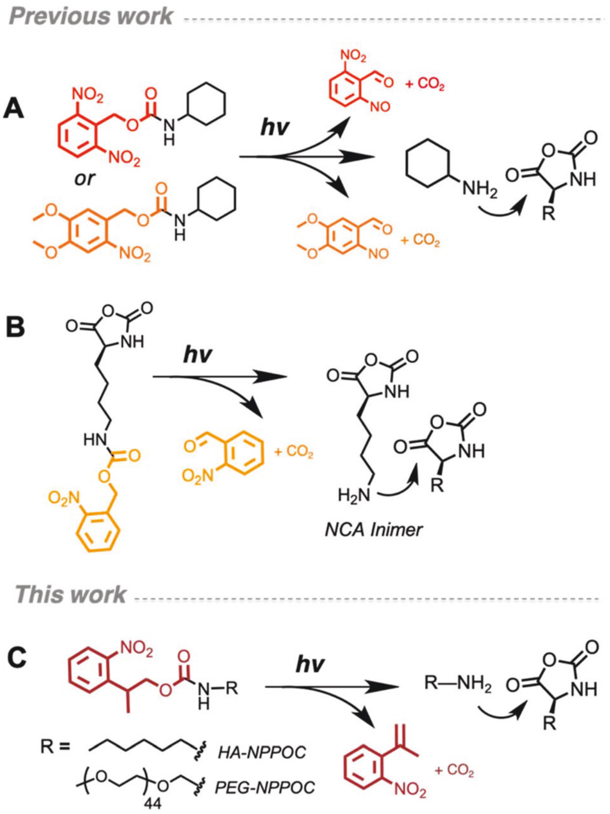

Fig. 1 Photoinitiated NCA ROP using 2-nitrobenzyl photocages. Previous reports (A and B) exhibited extended photodegradation times and nitroso-aldehyde byproducts. This work (C) shows increased photodegradation kinetics and enhanced molecular weight control by relying on 2-(2-nitrophenyl)propyloxycarbonyl-protected amines.

slow release of initiating amines.[20,21] Rather than achieving full deprotection, the light was switched off after 2–5 min to keep molecular weight and dispersity low, leading to limited molecular weight control and limited use-efficiency of the photoinitiator. Similarly, Dong *et al.*[21] reported that N_{ε}-(*o*-nitrobenzyloxycarbonyl)-L-lysine-NCA showed 70% deprotection in anhydrous DMF after 360 min of light irradiation and that imination side-reactions between the amine chain-ends and the nitrosobenzaldehyde occurred with increasing irradiation time, leading to imine-terminated chain ends. Therefore, we reasoned that there is an opportunity to build on these seminal reports to further enhance the level of kinetic and molecular weight control achievable during photo-initiated ROP of NCAs.

Despite the high quantum yields of the aforementioned 2-nitrobenzyl photocages, their deprotection rate is highly sensitive to specific reaction conditions such as the concentration of the photocage, the presence of functional groups, and the solvent.[23] Xie studied the quantum yields of 2-(2-nitrophenyl) propyloxycarbonyl (NPPOC) galactose photodeprotection in aqueous methanol, acetonitrile, and an acetonitrile solution of piperidine or 1,8-diazabicycloundec-7-ene (DBU) (0.05 M). Shorter photolysis times were observed for lower concentrations of NPPOC; in 10% water/90% methanol complete deprotection was achieved after 25 min for 10 mM NPPOC *versus* only 5 min for 0.1 mM NPPOC.[24] Importantly, most of the preceding literature has utilized water or wet solvents, which can enhance deprotection rates due to the stabilization of the *aci*-nitro intermediate formed during irradiation.[25] The conditions typical of NCA ROP, such as the use of anhydrous solvent, are thereby expected to affect the decomposition rate of the photoprotecting groups, a fact that may partially explain slow deprotection rates reported previously.[19–22]

We therefore sought to utilize a photocage that exhibited an even higher quantum yield and decay rate under light irradiation and that would degrade into innocuous byproducts to prevent reaction with the propagating amine chain end (*e.g.*, such as the imine formation reported previously).[21] Compared to the more commonly used 2-nitrobenzyl functional groups, NPPOC generally exhibits a higher quantum yield. The presence of a β-methyl group promotes rapid α-hydrogen abstraction by the photo-excited nitro group through an alternative photocleavage mechanism, resulting in an α-methyl styrene byproduct rather than an aldehyde or ketone byproduct.[26] The rapid deprotection of NPPOC compared to traditional 2-nitrobenzyl photolabile protecting groups has been exploited in the synthesis of DNA microarrays,[27] in the development of "photo-click" reactions reported by Bowman and coworkers,[28,29] and, more recently, in the photoinitiation of L-lactide by the Dove group.[30] We thus hypothesized that photoinitation of NCA ROP using NPPOC as a photolabile group would result in faster, more efficient release of nucleophilic amines, leading to greater control over molecular weight and access to narrow molecular weight distributions.

Herein, we utilize NPPOC-photocages to achieve greater control of photo-initiated NCA polymerizations for the preparation of synthetic polypeptides. Complete deprotection was achieved in 30 min of UV-irradiation, leading to enhanced control over molecular weight and molecular weight distribution. Addition of a small amount of the bulky base commonly referred to as "proton sponge", 1,8-bis(dimethylamino) naphthalene, suppressed the undesired photolysis pathway and enhanced control, likely due to the deprotonation of chain-ends, leading to a greater number of active chain-ends for polymerization.

Results and discussion

Kinetics of photodeprotection

NPPOC-caged amines were synthesized (Fig. S1–S3†) as photoinitiators for the light-initiated synthesis of linear and block copolypeptides, an approach we termed photo-liberation of amines for NCA ROP (PLANCA ROP) (Fig. 1C). As photodegradation and release rate rely heavily on reaction conditions (*e.g.*, solvent, concentration, light intensity),[23] we first monitored the degradation rate of NPPOC-protected hexyl amine (HA-NPPOC) in dry DMF at a concentration of 5 μM using a commercially available UV light source centered at 365 nm. Photodeprotection and release of HA was monitored by ^{1}H

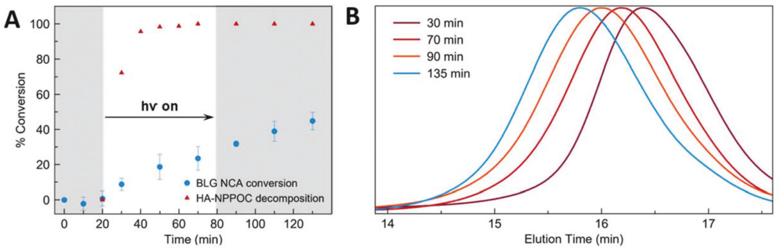

Fig. 2 Photo-liberation of hexylamine (HA) from 2-(2-nitrophenyl)propyloxycarbonyl-protected HA (HA-NPPOC) for polymerization of γ-benzyl-L-glutamate (BLG): (A) conversion *versus* time for the decomposition of HA-NPPOC and consumption of BLG NCA; (B) SEC traces of kinetic aliquots, demonstrating increasing MW with time; (C) experimental molecular weight (circles), theoretical molecular weight (dashed line), and molecular weight dispersity (diamonds) *versus* conversion. Molecular weights calculated from light scattering detection during SEC.

NMR spectroscopy. Release of HA was demonstrated to progress rapidly, with ~70% deprotection after 10 min and complete deprotection after 30 min of irradiation (Fig. S4†). We reasoned that the rapid release kinetics of HA-NPPOC would impart enhanced control in NCA ROP.

Efficacy of HA-NPPOC as a photoinitiator for NCA ROP

To test HA-NPPOC as a photoinitiator for NCA ROP, the polymerization of γ-benzyl-L-glutamate (BLG) NCA (Fig. S5†) in the presence of HA-NPPOC (Fig. S1†) was monitored under UV irradiation (BLG NCA : HA-NPPOC = 50 : 1, [BLG NCA] = 0.2 M in anhydrous DMF). Due to the dormancy of the photo-initiator, NCA, HA-NPPOC, and solvent could all be added to the reaction flask simultaneously. The reaction was monitored for 10 min in the dark, and no consumption of BLG NCA or decomposition of HA-NPPOC was observed. Upon light irradiation, HA-NPPOC rapidly degraded to release hexylamine, and consumption of BLG NCA became apparent as shown in Fig. 2A. The reaction was irradiated for 60 min to ensure complete decomposition of HA-NPPOC to release HA. Reaction kinetics demonstrated a shift to higher molecular weight (MW) with low molecular weight dispersity during the polymerization, as expected for NCA ROP proceeding through the normal amine mechanism (Fig. 2B). However, the resulting experimental molecular weights of poly(γ-benzyl-L-glutamate) (PBLG) were higher than expected (Fig. 2C). For example, at 48% conversion, the molecular weight was more than double the expected value ($M_{\text{n, actual}}$ = 12 300 g mol^{-1}, $M_{\text{n, theo}}$ = 5530 g mol^{-1}, $Đ$ = 1.3). Cooling the reaction by running compressed air over the reaction vessel to compensate for the heating that occurred during irradiation did not result in significant improvement of molecular weight control (Fig. S6†). We reasoned that the discrepancies in molecular weight may arise *via* two pathways: (1) slow initiation that would result from slow deprotection of the photocage, or (2) chain termination by the terminal amine reaction with the NPPOC degradation byproducts.

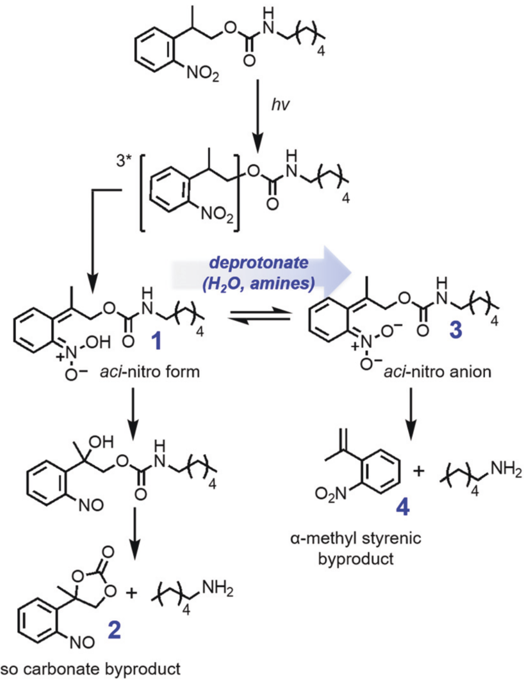

Fig. 3 Photodeprotection of NPPOC-containing compounds proceeding through two different pathways to produce either a nitroso carbonate (**2**) or an α-methyl styrenic byproduct (**4**).

Examination of the photodeprotection mechanism

In addition to the α-methyl styrenic byproduct (**4**), NPPOC can undergo an alternative deprotection mechanism as depicted in Fig. 3.[28] After photoexcitation, an intramolecular rearrangement deprotection pathway may proceed, resulting in a nitroso carbonate product (**2**). We reasoned that if such reactions are occurring early in the polymerization, higher than expected molecular weights would be observed. Furthermore, nitroso product (**2**) could act as an internal filter[28] due to its absorption in the range of the irradiation source.

Previous reports indicate NPPOC-protected compounds primarily undergo a β-elimination process to produce the α-methyl styrenic byproduct (**4**) (Fig. 3), with the reaction pathway being dependent on the solvent, substrate, and presence of bases. Bowman *et al.*[29] noted that NPPOC (0.05 mM in methanol) initially formed the nitroso carbonate by product (**2**) upon UV irradiation (320–390 nm) but eventually transitioned to primarily the β-elimination mechanism once hexylamine was released, likely due to hexylamine acting as a base to deprotonate the *aci*-nitro intermediate (**1**). It is therefore plausible that a propagating amine chain-end could react with the *aci*-nitro intermediate (**1**) to become protonated and lose its requisite nucleophilicity at room temperature.

NPPOC photolysis occurs most quickly under aqueous conditions; however, the presence of water is not suitable for conventional NCA ROP. Under anhydrous conditions, it has been shown that the presence of a base during light irradiation increases the deprotection rate and promotes the desired β-elimination pathway *via* deprotonation of the *aci*-nitro intermediate (**1**).[24,27] Yi *et al.* observed the suppression of the nitroso byproduct in the presence of 0.05 M DBU at the expense of a slightly increased half-life of 75 s compared to 35 s in 10% (v/v H_2O/MeOH).[24] Various bases at low concentrations have been demonstrated to be effective promoters in the deprotection of NPPOC. For the deprotection of phosphoramidites in the light-directed synthesis of oligonucleotides, DBU and *N*-diisopropylethylamine (DIPEA) were found to be especially effective at increasing the deprotection rate, presumably due to the rapid release of protected amine after deprotonation of the *aci*-nitro intermediate (**1**) to the *aci*-nitro anion (**3**).[27] Using concentrations of 0.05 M base, complete deprotection in anhydrous conditions was achieved in 5 min of light irradiation at 365 nm.[24,27]

Although NCAs polymerize in the presence of both nucleophilic and basic amines through the normal amine mechanism or the activated monomer mechanism, respectively, we hypothesized that the right combination of steric hindrance and basicity may promote the β-elimination photodeprotection pathway to form primarily the α-methyl styrenic byproduct, without initiating NCA polymerization to an appreciable extent. The addition of DBU has been shown to suppress the presence of nitroso byproducts; however, the concentration and strength of the base must be considered in order to avoid premature deprotection without light.[24,27] For our system, rapid deprotection is important to both enhance the rate of initiation and reduce the internal filter effect of any formed nitroso product. To test this approach, BLG NCA was incubated in anhydrous DMF with low concentrations (0.5 mM) of bases, including DBU, DIPEA, and proton sponge.[31] Proton sponge has been widely used in cationic polymerizations due to its high basicity and slow absorption of protons.[32] During incubation of the bases with the monomer, conventional polymerization occurred rapidly for DBU and DIPEA (Fig. S7†). Background initiation by the base would result in reduced molecular weight control and should be minimized to achieve targeted molecular weights. Fortunately, incubation of BLG NCA with proton sponge resulted in minimal polymerization of BLG NCA over 3 h.

We therefore investigated PLANCA ROP with HA-NPPOC and low concentrations of proton sponge under the same conditions outlined above. Initial reactions were performed with 0.1 equiv. of base to HA-NPPOC (BLG NCA : HA-NPPOC : proton sponge = 50 : 1 : 0.1, 0.4 mM base). Conventional NCA ROP initiated with hexyl amine and PLANCA ROP in the absence of base were performed for comparison. All PLANCA polymerizations were monitored using FT-IR spectroscopy and were incubated for 20 min before UV irradiation to ensure temporal control. As shown in Fig. 4, PLANCA ROP demonstrated slower polymerization kinetics and higher molecular weights compared to conventional NCA ROP with hexyl amine (Table 1, entries 1 and 2), suggesting fewer propagating centers were present in the photopolymerization. However, addition of 0.1 equiv. proton sponge increased the PLANCA photopolymerization rate, although the polymerizations remained slower than conventional NCA ROP, while maintaining temporal control as evident by the lack of polymerization prior to irradiation. At full monomer conversion, the observed molecular weights were slightly closer to the theoretical values (Table 1, entry 3) compared to polymerizations carried out in the absence of proton sponge (Table 1, entry 2). Increasing the amount of base to 0.2 equiv. further enhanced the polymerization rate compared to PLANCA without proton sponge (Fig. 4C) and resulted in M_n values even closer to the theoretical values (Table 1, entry 4). Further increasing the concentration of proton sponge to 0.5 equiv. resulted in premature polymerization of BLG NCA in the absence of light. Previous reports have also noted that higher concentrations of

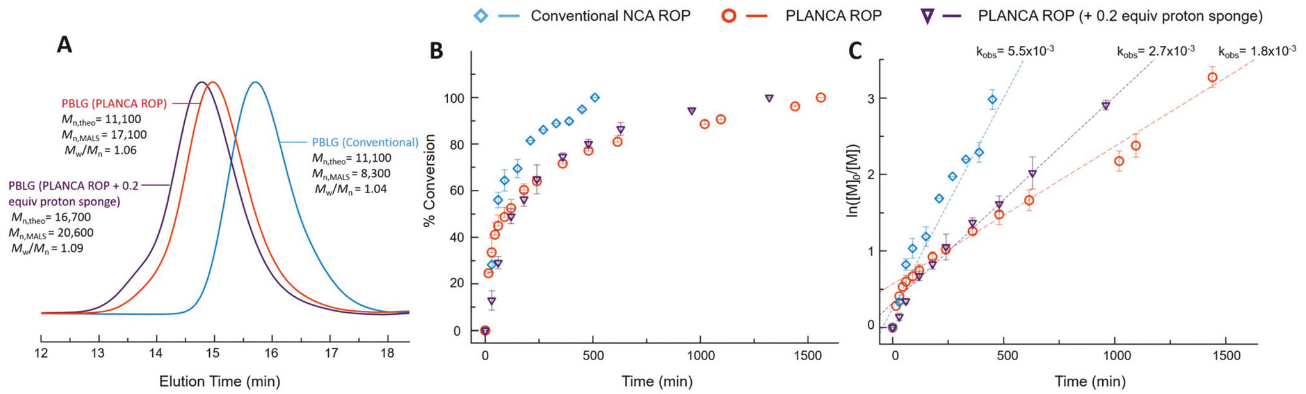

Fig. 4 (A) SEC traces at full monomer conversion, (B) monomer conversion *versus* time, and (C) pseudo-first-order kinetic plots for conventional NCA ROP, PLANCA ROP, and PLANCA ROP with 0.2 equiv. of proton sponge. Molecular weights calculated from light scattering detection during SEC.

Table 1 Conventional BLG-NCA and PLANCA ROP polymerizations

Entry	[BLG] : [Initiator] : [Base]	Initiator	Base	Conversion (%)	M_n, Theoretical	M_n, MALS (g mol^{-1})	Đ	M_n, PS Conv. Cal (g mol^{-1})	Đ
1	50 : 1 : 0	HA	—	100	11 100	10 200	1.01	10 900	1.13
2	50 : 1 : 0	HA-NPPOC	—	100	11 100	25 300	1.09	21 500	1.39
3	50 : 1 : 0.1	HA-NPPOC	Proton sponge	100	11 100	17 000	1.05	15 200	1.22
4	50 : 1 : 0	HA-NPPOC	—	50	5530	15 400	1.12	12 300	1.30
5	50 : 1 : 0.2	HA-NPPOC	Proton sponge	45	4970	10 100	1.18	9800	1.25
6	50 : 1 : 0	Entry 4	—	100	26 300	17 300	1.13	15 500	1.27
7	50 : 1 : 0	Entry 5	—	100	15 900	19 300	1.07	18 000	1.28
8	50 : 1 : 0.2	HA-NPPOC	Proton sponge	100	11 100	14 100	1.04	14 000	1.20
9	22 : 1 : 0	HA-NPPOC	—	100	4940	15 200	1.04	14 300	1.17
10	40 : 1 : 0	Entry 8	—	100	22 900	21 000	1.07	19 300	1.25
11	40 : 1 : 0	Entry 9	—	100	24 100	21 700	1.05	19 200	1.29
12	30 : 1 : 0	PEG-NPPOC	—	60	6460	15 800	1.33	13 300	1.56
13	30 : 1 : 0.2	PEG-NPPOC	Proton sponge	53	6000	9140	1.21	9490	1.28

Polymer molecular weights and molecular weight distributions were determined by size exclusion chromatography. Theoretical M_n calculated as follows: $[MW_{Macroinitiator}] + [(MW_{BLG}$ repeat unit$) \times ([BLG]/[Macroinitiator]) \times (Conversion)]$.

base (0.5 M) result in premature deprotection of NPPOC by the base alone.[27] Additionally, faster polymerizations were observed for PLANCA-ROP with 0.2 equiv. of proton sponge with increasing light intensity (Fig. S8†) and stir rate (Fig. S9†). We believe this is due to the increasing stir rate promoting more initiator availability early in the polymerization by overcoming the internal filter effects of the proton sponge that attenuates the light source.

The rate of initiator deprotection is slower in the presence of proton sponge (Fig. S4†) because the overlapping absorption wavelengths of proton sponge with NPPOC (Fig. S10†) attenuates the light *via* an internal filter effect that delays complete release of initiator during UV irradiation. Despite the slower initiation in the presence of proton sponge, once full initiator deprotection is achieved the propagation rate was enhanced, achieving a k_{obs} of 2.7×10^{-3} s^{-1} compared to 1.8×10^{-3} s^{-1} in the absence of proton sponge (Fig. 4C). Importantly, polymerizations in the presence of proton sponge demonstrated an increase in living chain-end retention (Fig. S11C†), which we attribute to the reduced likelihood of side reactions with the decomposition products of NPPOC formed during deprotection.

To gain further understanding into the PLANCA mechanism, MALDI-ToF-MS was used to analyze the resulting polymers of conventional NCA ROP, PLANCA ROP, and PLANCA ROP in the presence of 0.2 equiv. of proton sponge. The product of each polymerization was isolated by precipitation into cold ether prior to full conversion (Table 1, entries 4–11) and stored at 0 °C until MALDI-ToF-MS analysis (Table 1, entries 8–11). Fig. S11B† reveals that the PBLG derived from PLANCA ROP without proton sponge has a larger number of chain populations compared to PLANCA in the presence of proton sponge, *i.e.*, the presence of proton sponge reduces the populations of minor end-groups (Fig. S11C†). By comparing end-group molecular weight differences, potential side reactions and initiation pathways can be elucidated for the three polymerization methods. One distribution present in PLANCA polymerizations without proton sponge could potentially be attributed to Michael addition of the amine chain end with the α-methyl styrenic byproduct (Fig. S11B†), the reaction we tried to minimize by adding proton sponge. No Michael addition adducts were observed for PLANCA with proton sponge in the MALDI-ToF-MS spectra (Fig. S11C†). Polymer chains initiated by water were identified in PLANCA polymerizations with and without proton sponge. We believe that protonated chain-ends also contribute to chain-end termination, however this could not be detected by MALDI-ToF-MS. Overall, it is clear that PLANCA in the presence of small equivalences of proton sponge reduces chain-end reactions with NPPOC byproducts, producing more well-defined polypeptides with molecular weights closer to the theoretical values and narrower molecular weight distributions.

Active chain-end retention and chain extension

To evaluate the retention of active chain-ends of the resulting PLANCA ROP polymers, chain extension with BLG NCA was conducted. As chain-ends that have reacted with byproducts cannot initiate NCA-ROP, only active amine chain ends were expected to undergo chain-extension. Chain extension was performed on polymers that had been isolated after reaching 50% conversion (Table 1, entries 4 and 5) and complete conversion (Table 1, entries 8 and 9) to determine whether there was an increased extent of termination at higher conversions. As shown in Fig. 5A and Table 1, entry 6, chain-extension of PBLG (50% conversion) derived from PLANCA in the absence of base resulted in only a small shift to higher MW, indicating significant loss of chain-ends (Fig. 5A and Table 1, entry 6). Conversely, polymers prepared by PLANCA in the presence of proton sponge resulted in a clean chain-extension to higher MW (Fig. 5B and Table 1, entry 7). Some chain-end loss was observed for the macroinitiators obtained after full conversion; however, efficient extension was observed (Fig. S12 and S13†). As shown in Fig. 5A and Table 1, entry 6, chain-extension of PBLG derived from PLANCA in the absence of base resulted in only a small shift to higher MW, suggesting significant loss of chain-ends (Fig. S13A and S13B†). Conversely, polymers pre-

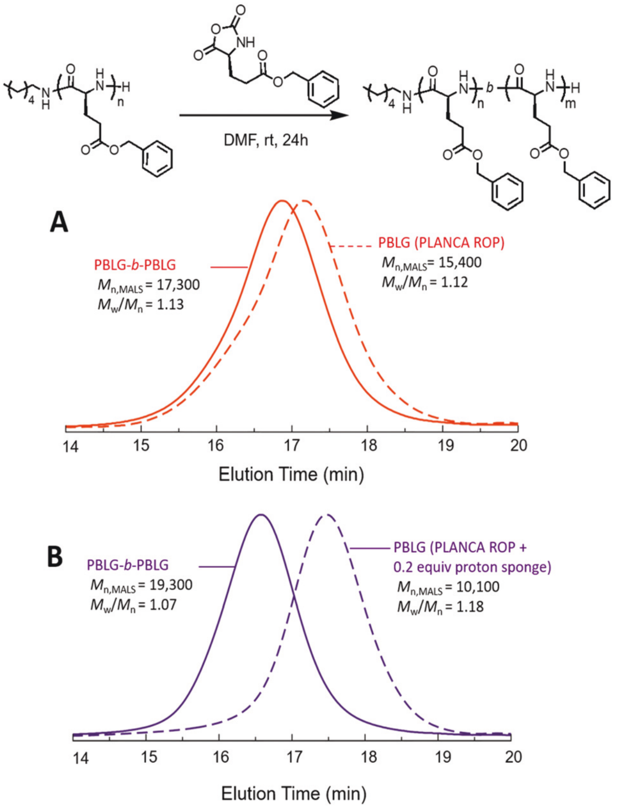

Fig. 5 Chain-extension of (A) PLANCA-derived PBLG (Table 1, entries 4 and 6), and (B) PLANCA + PS-derived PBLG (Table 1, entries 5 and 7). Dashed line – PBLG, solid line – PBLG-b-PBLG.

pared by PLANCA in the presence of proton sponge resulted in a clean chain-extension to higher MW (Fig. 5B and Table 1, entry 7). To our knowledge, this is the first demonstration of the ability to retain and extend active chain ends in light-initiated NCA polymerizations.

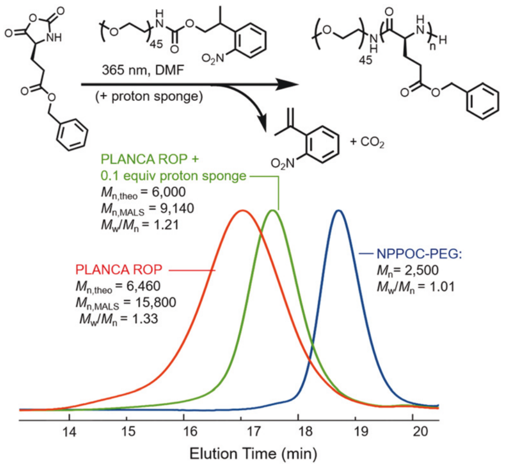

Fig. 6 Synthesis of polypeptide block copolymers by light, using PLANCA ROP with NPPOC-protected PEG-amine. Molecular weights determined from light scattering detection during SEC.

Photopolymerization of macroinitiator to form block copolypeptides

Lastly, the synthesis of polypeptide block copolymers under light was demonstrated using NPPOC-protected mPEG-amine (PEG-NPPOC) (Fig. S3 and S4†). Fig. 6 depicts the SEC traces of the block copolypeptides synthesized by PLANCA ROP using PEG-NPPOC with and without 0.2 equiv. of proton sponge (Table 1, entries 12 and 13). As expected, polymerization in the presence of proton sponge resulted in block copolymers with molecular weights closer to the theoretical values and with narrower molecular weight distributions. The ability to extend PLANCA to multi-block copolymers greatly expands its potential future use.

Conclusion

This polymerization approach using photodeprotectable amines affords excellent temporal control without sacrificing the narrow molecular weight distributions and MW control associated with conventional NCA polymerization. The use of NPPOC resulted in faster deprotection kinetics compared to other 2-nitrobenzyl photocages, as well as faster initiation, lower irradiation times, and narrower molecular weight distributions. The system was further improved through the addition of base, which increased the polymerization rate and produced more well-controlled polymerizations with active polypeptide chain-ends. We believe that the increased polymerization rate and higher chain-end retention in the presence of base is due to the promotion of the β-elimination pathway of NPPOC release. While we cannot fully eliminate the possibility that proton sponge may be slowly initiating NCA ROP through the activated monomer mechanism, the lack of polymerization in the absence of light suggests a relatively low contribution of initiation by the added base. Most importantly, we demonstrated the first successful chain-extension of polypeptides obtained from light-initiated polymerization and the synthesis of block copolypeptides using a PEG-based photoinitiator. Future work can be carried out to optimize photoinitiation of these systems, for instance through modification of NPPOC or the addition of a photosensitizer to increase its sensitivity. We believe this work has potential to be expanded into more complex photo-mediated biomaterial systems using photolithography and additive manufacturing.

Conflicts of interest

There are no conflicts to declare.

Acknowledgements

This material is based upon work partially supported by the National Science Foundation (DMR-1904631) (B. S. S.) and the

National Institute of Health (NIH S10 OD021758-01A1). Financial support from the Citrus Research Board of California is acknowledged.

Notes and references

1 M. Chen, M. Zhong and J. A. Johnson, *Chem. Rev.*, 2016, **116**, 10167–10211.

2 Q. Michaudel, V. Kottisch and B. P. Fors, *Angew. Chem., Int. Ed.*, 2017, **56**, 9670–9679.

3 R. N. Carmean, M. B. Sims, C. A. Figg, P. J. Hurst, J. P. Patterson and B. S. Sumerlin, *ACS Macro Lett.*, 2020, **9**, 613–618.

4 Y. Yagci, S. Jockusch and N. J. Turro, *Macromolecules*, 2010, **43**, 6245–6260.

5 S. Dadashi-Silab, S. Doran and Y. Yagci, *Chem. Rev.*, 2016, **116**, 10212–10275.

6 C. P. Kabb, C. S. O'Bryan, C. C. Deng, T. E. Angelini and B. S. Sumerlin, *ACS Appl. Mater. Interfaces*, 2018, **10**, 16793–16801.

7 R. A. Olson, A. B. Korpusik and B. S. Sumerlin, *Chem. Sci.*, 2020, 5142–5156.

8 J. Cheng and T. J. Deming, *Top. Curr. Chem.*, 2011, **310**, 1–26.

9 H. Lu, J. Wang, Z. Song, L. Yin, Y. Zhang, H. Tang, C. Tu, Y. Lin and J. Cheng, *Chem. Commun.*, 2014, **50**, 139–155.

10 H. Lu and J. Cheng, *J. Am. Chem. Soc.*, 2008, **130**, 12562–12563.

11 T. J. Deming, *Chem. Rev.*, 2015, **116**, 786–808.

12 J. Cao, P. Hu, L. Lu, B. A. Chan, B. H. Luo and D. Zhang, *Polym. Chem.*, 2015, **6**, 1226–1229.

13 H. Lu, J. Wang, Y. Bai, J. W. Lang, S. Liu, Y. Lin and J. Cheng, *Nat. Commun.*, 2011, **2**, 206–215.

14 N. P. Gabrielson, H. Lu, L. Yin, D. Li, F. Wang and J. Cheng, *Angew. Chem., Int. Ed.*, 2012, **51**, 1143–1147.

15 Y. Shen, X. Fu, W. Fu and Z. Li, *Chem. Soc. Rev.*, 2015, **44**, 612–622.

16 G. E. Negri and T. J. Deming, *ACS Macro Lett.*, 2016, **5**, 1253–1256.

17 L. Yin, H. Tang, K. H. Kim, N. Zheng, Z. Song, N. P. Gabrielson, H. Lu and J. Cheng, *Angew. Chem., Int. Ed.*, 2013, **52**, 9182–9186.

18 G. Liu and C.-M. Dong, *Biomacromolecules*, 2012, **13**, 1573–1583.

19 T. Stukenkemper, J. F. G. A. Jansen, C. Lavilla, A. A. Dias, D. F. Brougham and A. Heise, *Polym. Chem.*, 2017, **8**, 828–832.

20 T. Stukenkemper, X. Paquez, M. W. G. M. Verhoeven, E. J. M. Hensen, A. A. Dias, D. F. Brougham and A. Heise, *Macromol. Rapid Commun.*, 2018, **39**, 1700743.

21 P. Li and C. M. Dong, *ACS Macro Lett.*, 2017, **6**, 292–297.

22 P. Li, Y. Song and C. M. Dong, *Polym. Chem.*, 2018, **9**, 3974–3986.

23 P. Kla, T. Š. Olomek, C. G. Bochet, A. Blanc, R. Givens, M. Rubina, V. Popik, A. Kostikov and J. Wirz, *Chem. Rev.*, 2013, **113**, 119–191.

24 H. Yi, S. Maisonneuve and J. Xie, *Org. Biomol. Chem.*, 2009, **7**, 3847–3854.

25 M. Gaplovsky, Y. V. Il'ichev, Y. Kamdzhilov, S. V. Kombarova, M. Mac, M. A. Schwörer and J. Wirz, *Photochem. Photobiol. Sci.*, 2005, **4**, 33–42.

26 R. S. Foote, P. Cornwell, K. R. Isham, H. Gigerich, K.-P. Stengele, W. Pfleiderer and Ri. A. Sachleben, *Tetrahedron*, 1997, **53**, 4247–4264.

27 M. Beier and J. D. Hoheisel, *Nucleic Acids Res.*, 2000, **28**, e11.

28 W. Xi, M. Krieger, C. J. Kloxin and C. N. Bowman, *Chem. Commun.*, 2013, **49**, 4504–4506.

29 W. Xi, H. Peng, A. Aguirre-Soto, C. J. Kloxin, J. W. Stansbury and C. N. Bowman, *Macromolecules*, 2014, 6159–6165.

30 P. K. Kuroishi and A. P. Dove, *Chem. Commun.*, 2018, **54**, 6264–6267.

31 A. L. Llamas-Saiz, C. Foces-Foces and J. Elguero, *J. Mol. Struct.*, 1994, **328**, 297–323.

32 A. F. Pozharskii and V. A. Ozeryanskii, *Mendeleev Commun.*, 2012, **22**, 117–124.